J|A|C|S
ARTICLES
Published on Web 11/23/2004

Helical Aromatic Oligoamides: Reliable, Readily Predictable Folding from the Combination of Rigidified Structural Motifs

Lihua Yuan, Huaqiang Zeng, Kazuhiro Yamato, Adam R. Sanford, Wen Feng, Hanudatta S. Atreya, Dinesh K. Sukumaran, Thomas Szyperski, and Bing Gong*

Contribution from the Department of Chemistry, Natural Sciences Complex, University at Buffalo, The State University of New York, Buffalo, New York 14260

Received May 27, 2004; E-mail: bgong@chem.buffalo.edu

Abstract: Factors responsible for the folding of aromatic oligoamides with backbones rigidified by local three-center H-bonds were investigated. The stability of the three-center H-bonds was quantified by the half-lives of amide proton−deuterium exchange reactions, which show that the three-center H-bonds were largely intact at room temperature in the oligomer examined. This result is consistent with our current and previous 2D NMR studies. The overall helical conformation of nonamer **1** was found by variable-temperature NOESY studies to be dynamic. As temperature rose, the end-to-end NOEs rapidly disappeared, while the amide side chain NOEs were still readily detectable, corresponding to the "breath" and stretching of the helix by slightly twisting the local H-bonded rings. Based on the simple repetition of the same structural motif and local conformational preference, undecamer **2** was found to fold into well-defined helical conformation. The predictability of the folding of these backbone-rigidified aromatic oligoamides was demonstrated by a simple modeling method using structural parameters from oligomers with known crystal structures. The reliability and generality of the modeling methods were shown by the excellent agreement between the modeled structures corresponding to **1** and **2** and data from NOESY studies.

Introduction

Many unnatural oligomers that fold into well-defined secondary structures have been reported since the pioneering work of Gellman and Seebach on β-peptides.[1,2] Among reported examples, foldamers adopting various helical conformations have attracted the most attention.[3−6] Helical foldamers include β-peptides,[7,8] γ-peptides[9,10] δ-peptides,[11,12] and peptoid oligomers,[13] pyridine−pyrimidine oligomers and helical polyheterocyclic strands,[14] helicates,[15] oxapeptides,[16] *N*,*N*′-linked oligoureas,[17] and solvent-dependent helical oligo(phenylene ethynylenes).[18] Other foldamers involving unnatural backbones were also described.[19] In addition to folded oligomers, related systems based on the combination of inter- and intramolecular noncovalent interactions, particularly those involving the cooperative action of noncovalent forces, have also resulted in well-defined conformations.[20]

We[21] and others[22] recently described backbone-rigidified aromatic oligomers that fold into helical conformations. One class of the helical foldamers developed by us involve aromatic oligoamides whose backbones are rigidified by a novel set of three-center intramolecular H-bonds consisting of the S(5) and S(6) type[23] hydrogen-bonded rings. The localized three-center H-bonds, combined with rigid aromatic rings, lead to preferred, i.e., "locked" local conformations. The combination of these preferred local conformations results in an overall rigidified, crescent backbone for the corresponding oligomers. The rigidi-

(1) Appella, D. H.; Christianson, L. A.; Karle, I. L.; Powell, D. R.; Gellman, S. H. *J. Am. Chem. Soc.* **1996**, *118*, 13071.
(2) Seebach, D.; Overhand, M.; Kühnle, F. N. M.; Martinoni, B.; Oberer, L.; Hommel, U.; Widmer, H. *Helv. Chim. Acta* **1996**, *79*, 913.
(3) Sanford, A. R.; Gong B. *Curr. Org. Chem.* **2003**, *7*, 1649.
(4) Gong, B. *Chem. Eur. J.* **2001**, *7*, 4336.
(5) Huc, I. *Eur. J. Org. Chem.* **2004**, 17.
(6) Rowan, A. E.; Nolte, R. J. M. *Angew. Chem., Int. Ed.* **1998**, *37*, 63.
(7) Gellman, S. H. *Acc. Chem. Res.* **1998**, *31*, 173.
(8) Seebach, D.; Matthews, J. L. *Chem. Commun.* **1997**, 2015.
(9) (a) Hanessian, S.; Luo, X. H.; Schaum, R.; Michnick, S. *J. Am. Chem. Soc.* **1998**, *120*, 8569. (b) Hanessian, S.; Luo, X. H.; Schaum, R. *Tetrahedron Lett.* **1999**, *40*, 4925.
(10) Seebach, D.; Brenner, M.; Rueping, M.; Jaun, B. *Chem. Eur. J.* **2002**, *8*, 573.
(11) Szabo, L.; Smith, B. L.; McReynolds, K. D.; Parrill, A. L.; Morris, E. R.; Gervay, J. *J. Org. Chem.* **1998**, *63*, 1074.
(12) (a) Hungerford, N. L.; Claridge, T. D. W.; Watterson, M. P.; Aplin, R. T.; Moreno, A.; Fleet, G. W. J. *J. Chem. Soc., Perkin Trans. 1* **2000**, 3666. (b) Brittain, D. E. A.; Watterson, M. P.; Claridge, T. D. W.; Smith, M. D.; Fleet, G. W. J. *J. Chem. Soc., Perkin Trans. 1* **2000**, 3655.
(13) (a) Patch, J. A.; Barron, A. E. *J. Am. Chem. Soc.* **2003**, *125*, 12092. (b) Sanborn, T. J.; Wu, C. W.; Zuckerman, R. N.; Barron, A. E. *Biopolymers* **2002**, *63*, 12. (c) Wu, C. W.; Sanborn, T. J.; Huang, K.; Zuckermann, R. N.; Barron, A. E. *J. Am. Chem. Soc.* **2001**, *123*, 6778. (d) Armand, P.; Kirshenbaum, K.; Goldsmith, R. A.; Farr-Jones, S.; Barron, A. E.; Truong, K. T.; Dill, K. A.; Mierke, D. F.; Cohen, F. E.; Zuckermann, R. N.; Bradley, E. K. *Proc. Natl. Acad. Sci. U.S.A.* **1998**, *95*, 4309. (e) Kirshenbaum, K.; Barron, A. E.; Goldsmith, R. A.; Armand, P.; Bradley, E. K.; Truong, K. T.; Dill, K. A.; Cohen, F. E.; Zuckermann, R. N. *Proc. Natl. Acad. Sci. U.S.A.* **1998**, *95*, 4303.
(14) (a) Cuccia, L. A.; Ruiz, E.; Lehn, J.-M.; Homo, J.-C.; Schmutz, M. *Chem.-Eur. J.* **2002**, *8*, 3448. (b) Cuccia, L. A.; Lehn, J.-M.; Homo, J.-C.; Schmutz, M. *Angew. Chem., Int. Ed.* **2000**, *39*, 233. (c) Ohkita, M.; Lehn, J.-M.; Baum, G.; Fenske, D. *Chem. Eur. J.* **1999**, *5*, 3471. (d) Hanan, G. S.; Lehn, J.-M.; Kyritsakas, N.; Fischer, J. *J. Chem. Soc., Chem. Commun.* **1995**, 765.
(15) (a) Garrett, T. M.; Koert, U. Lehn, J.-M.; Rigault, A.; Meyer, D.; Fischer, J. *J. Chem. Soc., Chem. Commun.* **1990**, 557. (b) Lehn, J. M. *Supramolecular Chemistry*; VCH: Weinheim, Germany, 1995, and references therein. (c) Lehn, J.-M.; Rigault, A. *Angew. Chem., Int. Ed.* **1988**, *27*, 1095.
(16) (a) Yang, D.; Qu, J.; Li, B.; Ng, F.-F. Wang, X.-C.; Cheung, K.-K.; Wang, D.-P.; Wu, Y.-D. *J. Am. Chem. Soc.* **1999**, *121*, 589. (b) Wu, Y. D.; Wang, D. P.; Chan, K. W. K.; Yang, D. *J. Am. Chem. Soc.* **1999**, *121*, 11189.
(17) Semetey, V.; Rognan, D.; Hemmerlin, C.; Graff, R.; Briand, J. P.; Marraud, M.; Guichard, G. *Angew. Chem., Int. Ed.* **2002**, *41*, 1893.

10.1021/ja046858w CCC: $27.50

fied backbone forces an oligomer of a sufficient length to adopt a helical conformation containing a large, hydrophilic interior cavity. Our previous results revealed that the helical conformation was present both in solution and in solid state. The folded structures were independent of the nature of the side chains carried by the corresponding oligomers. Despite their rigidity, the folded conformations of these oligoamides are effected by reversible intramolecular H-bonding interactions. These oligomers are therefore true foldamers that should undergo dynamic exchange between folded and partially folded (or even unfolded) states as environmental factors such as temperature and solvent change. To use these backbone-rigidified folding oligomers as reliable, shape-persistent molecular building blocks for constructing large nanostructures, it is necessary to understand the stability of their folded conformations. For example, although we previously found that the three-center H-bonds were stabilized by positive cooperativity, it is still not clear how these three-center H-bonds, which play the critical role of defining the local conformational preference, would differ in their stabilities when placed in different locations along the backbone of a folded oligomer. What is the effect of temperature change on the overall folded conformation of an oligomer? Another concern about these oligomers is related to their H-bond-rigidified backbones. Is it possible that in long oligomers, the steric hindrance becomes so severe that some of the backbone-rigidifying intramolecular H-bonded rings will be broken, leading to interruption of the H-bonded crescent and helical conformations? Finally, since long oligomers are constructed by simple repetition of the same structural motif and local conformational preference, is it possible to accurately predict the folded conformations of long oligomers based on structural data from their shorter homologues?

In this paper, we first describe a method for quantifying the stability of the local three-center H-bonds based on the determination of the half-lives of amide proton−deuterium exchange. We then investigate the effect of temperature changes on the folded helical conformation of nonamer (9-mer) **1**. To probe the effect of chain length on folded conformations, we synthesized and characterized undecamer (11-mer) **2**. Results from extensive NMR studies suggest that this longer oligomer still adopts H-bond enforced, helical conformations. Finally, we have developed a modeling method for predicting the folded structures of oligomers **1b** and **2b** based on data from the crystal structures of short oligoamides. The reliability of the modeled structures was shown by their excellent agreement with results from two-dimensional (2D) nuclear Overhauser enhancement spectroscopy (NOESY) studies.

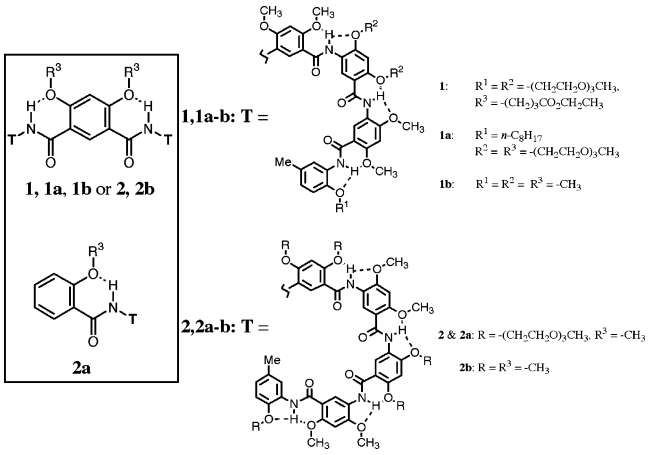

Results and Discussion

Synthesis. The synthesis of nonamer **1a** was reported by us before.[21d] Nonamer **1** was synthesized on the basis of the same procedures for synthesizing **1a** and other similar 9-mers. The symmetrical 11-mer **2**, consisting of a central isophthalic acid residue and two identical oligoamide "arms", was synthesized on the basis of a convergent route by coupling the corresponding 4,6-disubstituted isophthaloyl chlorides with the amino-terminated pentamer (Scheme 1a). Hexamer **2a** was similarly prepared by acylating the amino-terminated pentamer with

(18) (a) Goto, H.; Heemstra, J. M.; Hill, D. J.; Moore, J. S. *Org. Lett.* **2004**, *6*, 889. (b) Heemstra, J. M.; Moore, J. S. *Org. Lett.* **2004**, *6*, 659. (c) Heemstra, J. M.; Moore, J. S. *J. Am. Chem. Soc.* **2004**, *126*, 1648. (d) Stone, M. T.; Moore, J. S. *Org. Lett.* **2004**, *6*, 469. (e) Oh, K.; Jeong, K. S.; Moore, J. S. *J. Org. Chem.* **2003**, *68*, 8397. (f) Cary, J. M.; Moore, J. S. *Org. Lett.* **2002**, *4*, 4663. (g) Matsuda, K.; Stone, M. T.; Moore, J. S. *J. Am. Chem. Soc.* **2002**, *124*, 11836. (h) Zhao, D. H.; Moore, J. S. *J. Am. Chem. Soc.* **2002**, *124*, 9996. (i) Hill, D. J.; Moore, J. S. *Proc. Natl. Acad. Sci. U.S.A.* **2002**, *99*, 5053. (j) Tanatani, A.; Hughes, T. S.; Moore, J. S. *Angew. Chem., Int. Ed.* **2001**, *41*, 325. (k) Oh, K.; Jeong, K. S.; Moore, J. S. *Nature* **2001**, *414*, 889. (l) Prince, R. B.; Moore, J. S.; Brunsveld, L.; Meijer, E. W. *Chem.-Eur. J.* **2001**, *7*, 4150. (m) Brunsveld, L.; Meijer, E. W.; Prince, R. B.; Moore, J. S. *J. Am. Chem. Soc.* **2001**, *123*, 7978. (n) Tanatani, A.; Mio, M. J.; Moore, J. S. *J. Am. Chem. Soc.* **2001**, *123*, 1792. (o) Lahiri, S.; Thompson, J. L.; Moore, J. S. *J. Am. Chem. Soc.* **2000**, *122*, 11315. (p) Mio, M. J.; Prince, R. B.; Moore, J. S.; Kuebel, C.; Martin, D. C. *J. Am. Chem. Soc.* **2000**, *122*, 6134. (q) Yang, W. Y.; Prince, R. B.; Sabelko, J.; Moore, J. S.; Gruebele, M. *J. Am. Chem. Soc.* **2000**, *122*, 3248. (r) Prince, R. B.; Barnes, S. A.; Moore, J. S. *J. Am. Chem. Soc.* **2000**, *122*, 2758. (s) Prest, P. J.; Prince, R. B.; Moore, J. S. *J. Am. Chem. Soc.* **1999**, *121*, 5933. (t) Prince, R. B.; Saven, J. G.; Wolynes, P. G.; Moore, J. S. *J. Am. Chem. Soc.* **1999**, *121*, 3114. (u) Gin, M. S.; Yokozawa, T.; Prince, R. B.; Moore, J. S. *J. Am. Chem. Soc.* **1999**, *121*, 2643. (v) Prince, R. B.; Okada, T.; Moore, J. S. *Angew. Chem., Int. Ed.* **1999**, *38*, 233. (w) Nelson, J. C.; Saven, J. G.; Moore, J. S.; Wolynes, P. G. *Science* **1997**, *277*, 1793.

(19) (a) Gabriel. G. J.; Iverson, B. L. *J. Am. Chem. Soc.* **2002**, *124*, 15174. (b) Zych, A. J.; Iverson, B. L. *J. Am. Chem. Soc.* **2000**, *122*, 8898. (c) Nguyen, J. Q.; Iverson, B. L. *J. Am. Chem. Soc.* **1999**, *121*, 2639. (d) Lokey, R. S.; Iverson, B. L. *Nature* **1995**, *375*, 303. (e) Nowick, J. S.; Cary, J, M.; Tsai, J. H. *J. Am. Chem. Soc.* **2001**, *123*, 5176. (f) Nowick, J. S.; Mahrus, S.; Smith, E. M.; Ziller, J. W. *J. Am. Chem. Soc.* **1996**, *118*, 1066. (g) Hagihara, M.; Anthony, N. J.; Stout, T. J.; Clardy, J.; Schreiber, S. L. *J. Am. Chem. Soc.* **1992**, *114*, 6568. (h) Gennari, C.; Salom, B.; Potenza, D.; Williams, A. *Angew. Chem., Int. Ed. Engl.* **1994**, *33*, 2067. (i) Cho, C. Y.; Moran, E. J.; Cherry, S. R.; Stephans, J. C.; Fodor, S. P.; Adams, C. L.; Sundaram, A.; Jacobs, J. W.; Schultz, P. G. *Science* **1993**, *261*, 1303. (j) Smith, A. B., III; Keenan, T. P.; Holcomb, R. C.; Sprengeler, P. A.; Guzman, M. C.; Wood, J. L.; Carroll, P. J.; Hirschmann, R. *J. Am. Chem. Soc.* **1992**, *114*, 10672. (k) Winkler, J. D.; Piatnitski, E. L.; Mehlmann, J.; Kasparec, J.; Axelsen, P. H. *Angew. Chem., Int. Ed.* **2001**, *40*, 743. (l) Jones, T. V.; Blatchly, R. A.; Tew, G. N. *Org. Lett.* **2003**, *5*, 3297.

(20) (a) Zeng, H. Q.; Yang, X. W.; Brown, A. L.; Martinovic, S.; Smith, R. D.; Gong, B. *Chem. Commun.* **2003**, 1556. (b) Zeng, H. Q.; Ickes, H.; Flowers, R. A.; Gong, B. *J. Org. Chem.* **2001**, *66*, 3574. (c) Zeng, H. Q.; Yang, X. W.; Flowers, R. A.; Gong, B. *J. Am. Chem. Soc.* **2002**, *124*, 2903. (d) Hirschberg, J. H. K. K.; Brunsveld, L.; Ramzi, A.; Vekemans, J. A. J. M.; Sijbesma, R. P.; Meijer, E. W. *Nature* **2000**, *407*, 167. (e) Prins, L. J.; De Jong, F.; Timmerman, P.; Reinhoudt, D. N. *Nature* **2000**, *408*, 181.

(21) (a) Yang, X. W.; Yuan, L. H.; Yamato, K.; Brown, A. L.; Feng, W.; Furukawa, M.; Zeng, X. C.; Gong, B. *J. Am. Chem. Soc.* **2004**, *126*, 3148. (b) Yang, X. W.; Martinovic, S.; Smith, R. D.; Gong, B. *J. Am. Chem. Soc.* **2003**, *125*, 9932. (c) Yang, X. W.; Brown, A. L.; Furukawa, M.; Li, S.; Gardinier, W. E.; Bukowski, E. J.; Bright, F. V.; Zheng, C.; Zeng, X. C.; Gong. B. *Chem. Commun.* **2003**, 56. (d) Gong, B.; Zeng, H. Q.; Zhu, J. Yuan L. H.; Han, Y. H.; Cheng, S. Z.; Furukawa, M.; Parra, R. D.; Kovalevsky, A. Y.; Mills, J. L.; Skrzypczak-Jankun, E.; Martinovic, S.; Smith, R. D.; Zheng, C.; Szyperski, T.; Zeng, X. C. *Proc. Natl. Acad. Sci. U.S.A.* **2002**, *99*, 11583. (e) Parra, R. D.; Zeng, H. Q.; Zhu, J.; Zheng, C.; Zeng, X. C.; Gong, B. *Chem.-Eur. J.* **2001**, *7*, 4352. (f) Parra, R. D.; Furukawa, M.; Gong, B.; Zeng. X. C. *J. Chem. Phys.* **2001**, *115*, 6030. (g) Parra, R. D.; Gong, B.; Zeng. X. C. *J. Chem. Phys.* **2001**, *115*, 6036. (h) Zhu, J.; Parra, R. D.; Zeng, H.; Skrzypczak-Jankun, E.; Zeng, X. C.; Gong, B. *J. Am. Chem. Soc.* **2000,** *122*, 4219.

(22) (a) Hamuro, Y.; Geib, S. J.; Hamilton, A. D. *J. Am. Chem. Soc.* **1997**, *119*, 10587. (b) Berl, V.; Khoury, R. G.; Huc, I.; Krische, M. J.; Lehn, J.-M. *Nature* **2000**, *407*, 720. (c) Huc, I.; Maurizot, V.; Gornitzka, H.; Leger, J. M. *Chem. Commun*. **2002,** 578. (d) Jiang, H.; Leger, J. M.; Huc, I. *J. Am. Chem. Soc.* **2003**, *125*, 3448. (e) Jiang, H.; Léger, J.-M.; Dolain, C.; Guionneau, P.; Huc, I. *Tetrahedron* **2003**, *59*, 8365. (f) Jiang, H.; Dolain, C.; Leger, J. M.; Gornitzka, H.; Huc, I. *J. Am. Chem. Soc.* **2004**, *126*, 1034.

(23) Berstein, J.; Davis, R. E.; Shimoni, L.; Chang, N.-L. *Angew. Chem., Int. Ed. Engl.* **1995**, *34*, 1555.

Scheme 1

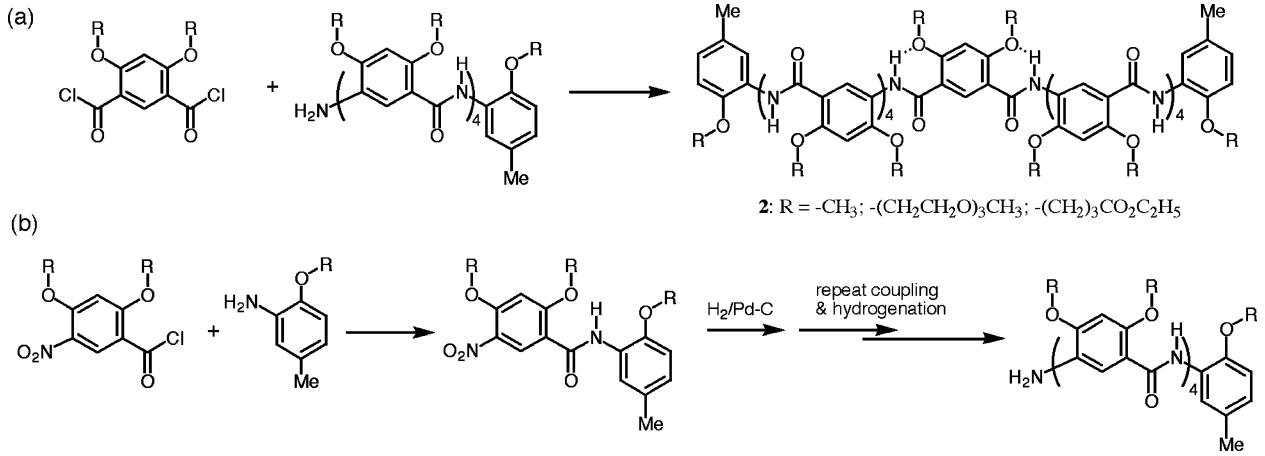

2-methoxybenzoyl chloride. The amino oligoamides were synthesized by stepwise (C-to-N) coupling of the corresponding monomer building blocks on the basis of acid chloride chemistry (Scheme 1b). The yield of each amide formation step ranged from 72 to 87%. Except for the first aniline residue, the other monomers were incorporated via nitrobenzoic acid chlorides. The resulting nitro-terminated oligoamide intermediates were hydrogenated (Pd/C) into the corresponding amino-terminated analogues, which were then subjected to the next coupling step. Hydrogenation of the nitro-terminated oligoamides was usually carried out at 40−55 °C under pressure (4 Pa) in chloroform/ethanol (2:1) for 4 h.

Amide Proton−Deuterium Exchange. Previous NOESY studies on our folding aromatic oligoamides clearly demonstrated the presence and persistence of the three-center H-bonds that played the critical role in enforcing the local conformational preference on the repeating structural motifs.[21d,e,h] To quantitatively measure the stability of these three-center H-bonds, H−D exchange experiments were performed on the previously characterized nonamer (9-mer) **1a**[21d] and dimers **3**, **3a**, and **3b**.[21e] The half-lives of H−D exchange for the amide protons are indicated in Figure 1. Consistent with the greatly enhanced stability of its corresponding three-center H-bond, dimer **3** showed a much longer half-life of amide H−D exchange than dimers **3a** and **3b**, each containing only two-center H-bonds. Dimer **3a**, with a six-membered H-bonded ring, was found to be slightly more resistant toward H−D exchange than **3b** with a five-membered H-bonded ring. The amide protons of **1a** showed half-lives of H−D exchange that were comparable or much longer than that of **3**, indicating that all of the amide protons in **1a** were involved in strong three-center H-bonding. The existence of three-center H-bonds suggests that each of the amide linkages in 9-mer **1a** was rigidified, enforcing a conformational preference that results in a tapelike, helical backbone. The half-lives of H−D exchange also provided a convenient comparison on the relative stabilities of the individual three-center H-bonds. For example, amide proton *d* of **1a** was found to exchange more easily than the other amide protons, indicating that the corresponding amide group was the weak point along the backbone of this 9-mer. This is consistent with both the crystal structure of a similar 9-mer previously determined by us and the results from theoretical calculations on an oligomer

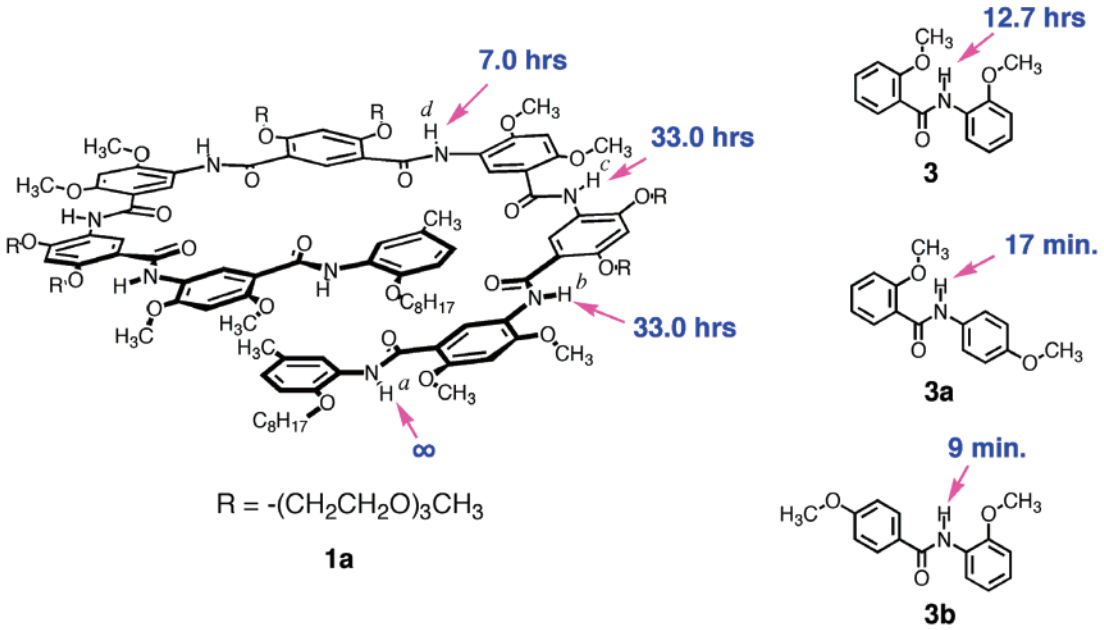

Figure 1. Half-lives of amide proton−deuterium exchange based on 1D NMR experiments (500 MHz, $CDCl_3$/DMSO-d_7/D_2O = 2:19:19).

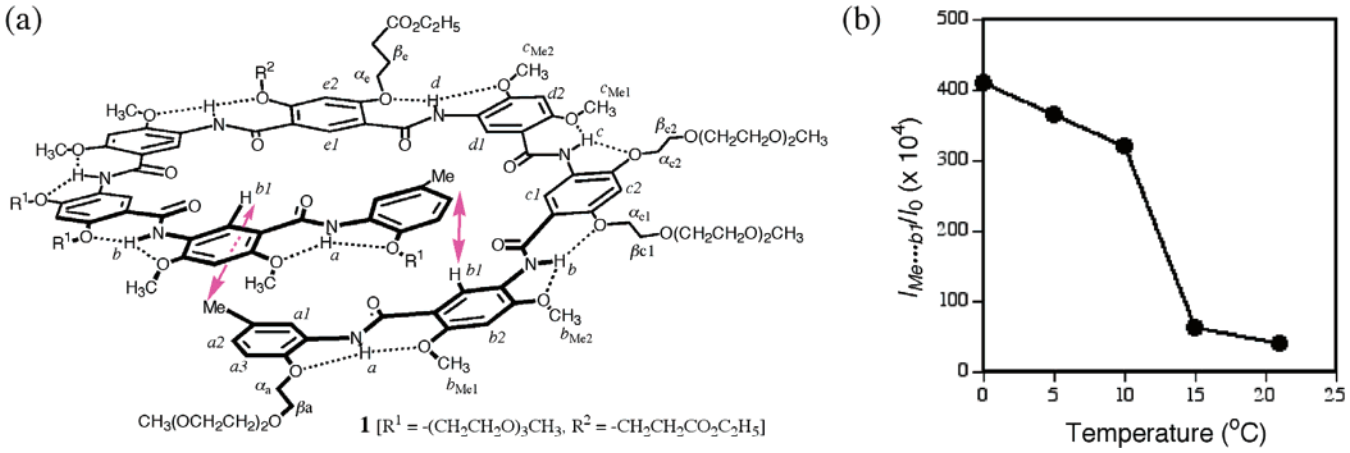

1 [R^1 = -$(CH_2CH_2O)_3CH_3$, R^2 = -$CH_2CH_2CO_2C_2H_5$]

Figure 2. (a) Two identical end-to-end NOEs (red arrows) of **1** followed by variable-temperature NOESY experiments (2 mM in $CDCl_3$; 500 MHz; mixing time, 140−500 ms). (b) The results show a rapid decrease in the intensity of the end-to-end NOEs as temperature rises.

involving a central isophthalic acid residue.[21d] The ability to follow the strength of an individual three-center H-bond should also facilitate studies on the inermolecular stacking interaction of these folding aromatic oligoamides.

Variable-Temperature 2D NMR (NOESY) Experiments. The effect of temperature on the folded conformation of **1** was investigated by variable-temperature NOESY experiments. The end methyl group (Me) serves as a convenient spectroscopic label for assigning the 2D NMR spectra. Results from our previous studies on similar symmetrical nonamers indicated that the two identical NOE contacts between the protons of the end methyl group and aromatic proton b1 could serve as a direct indicator for the corresponding helical conformation.[21d] Indeed, an obvious NOE between protons of Me and proton b1 was observed in the NOESY spectrum of **1** (Figure 2a). To examine the dynamic nature of the folded conformation of **1**, the temperature-dependent changes of the intensity of Me···b1 contact were followed.

Due to the influence of factors such as temperature and mixing time on the NOE intensities (integrated volumes) of a specific contact, NOEs measured at different temperatures cannot be directly compared. To correlate the changes of NOE intensities with conformational mobility or flexibility, the average intensity (I_0) of the NOEs between protons Me and their neighboring aromatic protons a1 and a2 was chosen as the internal standard:

$$I_0 = \frac{I_{Me\cdots a1} + I_{Me\cdots a2}}{2}$$

Since the average distances between the Me protons and protons a1 and a2 are fixed in the covalent structure, any observed changes of I_0 from NMR experiments carried out in the same solvent should be due to experimental conditions, such as temperature and mixing times. Thus, any NOE (I) measured simultaneously with I_0 should be subjected to the same influence of experimental conditions. Comparing the ratio I/I_0 measured at various temperatures and mixing times should provide a more accurate indicator for any conformation-dependent changes in I.

If the distance between protons Me and b1 were unaffected by temperature, the ratio $I_{Me\cdots b1}/I_0$ would remain largely unchanged as temperature varies. A much more likely scenario is that $I_{Me\cdots b1}$ will be affected by temperature-dependent conformational changes that cause the Me···b1 distance to change. As temperature rises, it is expected that the helical conformation of **1** will become increasingly dynamic, due to the temperature-dependent changes associated with the torsional angles of each of the numerous amide−aryl single bonds. Correspondingly, the average distance between the protons Me and b1 will also fluctuate more rapidly at higher temperatures. As a result, $I_{Me\cdots b1}$ will decrease rapidly and the ratio $I_{Me\cdots b1}/I_0$ will reflect the corresponding conformational dynamics. Indeed, results from NOESY experiments (500 MHz, in $CDCl_3$) indicated that the NOEs between protons Me and b1 diminished rapidly as temperature rose from 0 to 21 °C. This end-to-end (Me···b1) contact disappeared completely when temperature rose above 30 °C. As shown in Figure 2b, the ratio $I_{Me\cdots b1}/I_0$ at 21 °C is less than 10% of that at 0 °C. Considering that the measured intensity of I_0 at 21 °C is still 78% of that measured at 0 °C, the decrease of the intensity of $I_{Me\cdots b1}$ at elevated temperatures was very dramatic and indicated the dynamic nature of the helical conformation of **1**, which is equivalent to an increase in the average distance between the protons and reflects the "breath" and elongation of the helix.

The temperature-dependent conformational flexibility of **1** is further confirmed by examining the NOEs between amide protons *a* and *c* with their adjacent ether side chains. Two sets of NOEs associated with proton *a* or *c* were monitored: one set ($I_{S(6)}$) are those between the amide proton and the methyl or α-methylene protons of the side chains involved in the six-membered H-bonded rings (Figure 3a), and the other set ($I_{S(5)}$) are those between the amide hydrogen and the methyl or α-methylene protons of the chains involved in the five-membered H-bonded rings (Figure 3b). The temperature-dependent trend revealed by the amide group−side chain contacts is consistent with that of the end-to-end contact: the relative NOE intensities (I/I_0) dropped as temperature rose, suggesting that the helical conformation became increasingly dynamic as temperature rose. However, compared to the end-to-end NOE ($I_{Me\cdots b1}$), the localized amide−side chain NOEs ($I_{S(6)}$ and $I_{S(6)}$) decreased much more slowly. For example, at 30 °C, $I_{S(5)}$ and $I_{S(6)}$ could still be clearly detected, while $I_{Me\cdots b1}$ completely disappeared. It is also noticeable that $I_{S(6)}$ decreased more slowly than $I_{S(5)}$, suggesting the S(5) ring is the weaker of the two two-center components in a three-center H-bond.

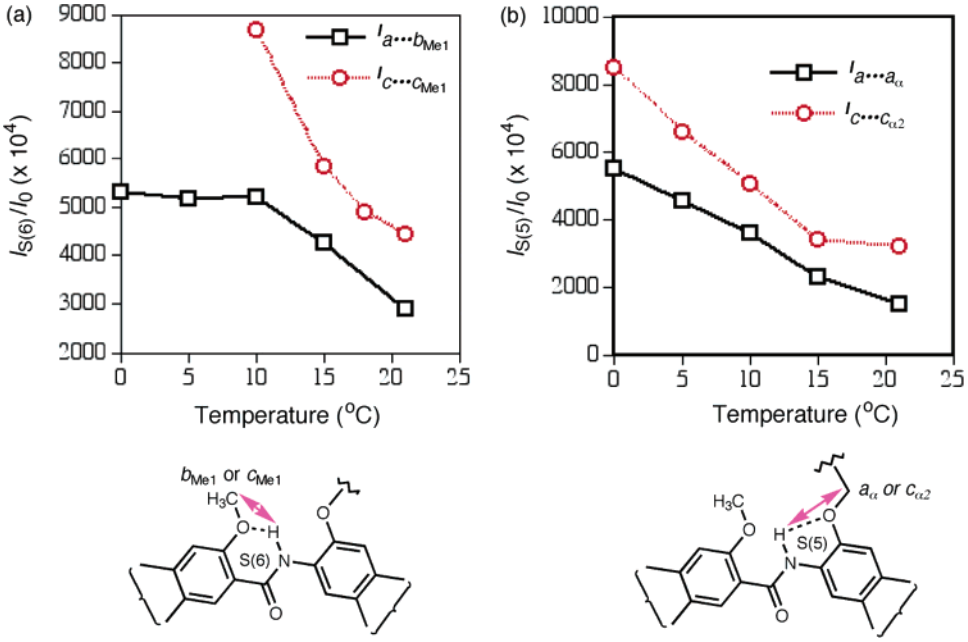

Figure 3. Temperature-dependent changes of the relative intensities of the NOEs between amide proton a or c and the protons on its neighboring side chains.

Thus, the temperature-dependent changes of the measured I/I_0 values were fully consistent with the H-bond-enforced, helical conformation of nonamer **1**: the end-to-end (Me···b1) contact was affected by the accumulative effect of conformational changes that resulted from all of the local H-bonded rings and was thus the most sensitive. At elevated temperatures, the less stable S(5) type intramolecularly hydrogen bonded rings were twisted more easily than the more stable S(6) type rings. As temperature kept rising, the N−Ph bond, as part of the S(5) ring, was the first to rotate freely, which should eventually lead to a completely random coil conformation of nonamer **1**. Given the fact that, as temperature rises, the end-to-end NOE disappears much more rapidly than the amide proton−side chain contacts, the helical structure of **1** probably breathes and extends such as a spring as the H-bonded rings distort.

Characterization of 11-mer 2. To probe whether an oligomer longer than nonamers can still fold into a helical structure, we designed and synthesized 11-mer **2**.

(1) One-Dimensional ^{1}H NMR Spectroscopy. The assignments of the 1D ^{1}H NMR spectrum of **2** and hexamer **2a** were aided by the COSY and NOESY spectra of these two oligomers. Figure 4 shows that the partial 1D NMR spectra of **2** and **2a** correspond to the range containing the amide and aromatic signals. The presence of sharp signals in both spectra is consistent with the well-defined and stable conformations adopted by these two oligomers. Although **2** and **2a** have the same residues that are connected in the same order, compared to those of **2a**, which can be regarded as half of **2**, the ^{1}H NMR signals of **2** are more widely dispersed. For example, the signals of the five interior aromatic protons of **2**, Ha1 to Hf1, are completely resolved. This confirms that **2** adopts a folded conformation that places its amide and aromatic protons in microenvironments different from those in **2a**. Most of the amide and aromatic signals of **2** shifted to upfield positions as compared to those of **2a**, which may be due to both the intramolecularly overlapped (or stacked) residues (see below) and the strong intermolecular aromatic stacking interactions of **2** due to its large aromatic surfaces.

(2) Two-Dimensional ^{1}H NMR Spectroscopy (NOESY). The conformation of 11-mer **2** was characterized by NOESY studies. The presence of the three-center H-bonds along the backbone of **2** should be revealed by three NOE contacts between each of the amide protons and the protons on its adjacent side chains. The three NOEs include one with the methoxy and two with the (α and *β*) methylene groups (Figure 5). Although the methoxy and *O*-methylene ^{1}H NMR signals cannot be clearly assigned due to the overlap of signals, three of the five amide proton NMR signals of **2** are well-resolved, which should lead to well-separated NOE cross-peaks in the 2D spectrum. Figure 5 shows the partial NOESY spectrum corresponding to the amide−alkoxy side chain NOEs of **2**. For the well-resolved amide protons a, b, and e, the expected NOEs were clearly detected. Each of protons b and e exhibited three well-separated cross-peaks with the OCH_3 and OCH_2 regions. Proton a showed two cross-peaks, one of which corresponded to a single NOE and the other should corresponded to two NOEs on the basis of its intensity. The signals of protons b and d, which are placed in very similar environments, partially overlapped. Correspondingly, three intense NOE cross-peaks for b and d were detected. The intensity of these NOE peaks, by comparing to those of the well-resolved protons b and e, suggested that each of these three cross-peaks corresponded to two overlapped NOEs, consistent with the overlap of the b and d signals. Thus, the observed NOEs between each of the amide protons of **2** and its neighboring protons on the two adjacent side chains are fully consistent with the presence of the three-centered H-bonds that rigidified the amide groups, which in turn should lead to an overall curved and helical conformation of **2**.

While the presence of strong NOEs between the amide protons and those of their neighboring side chains provided direct evidence for a H-bond rigidified backbone of **2**, the most conclusive evidence for the adoption of a helical conformation

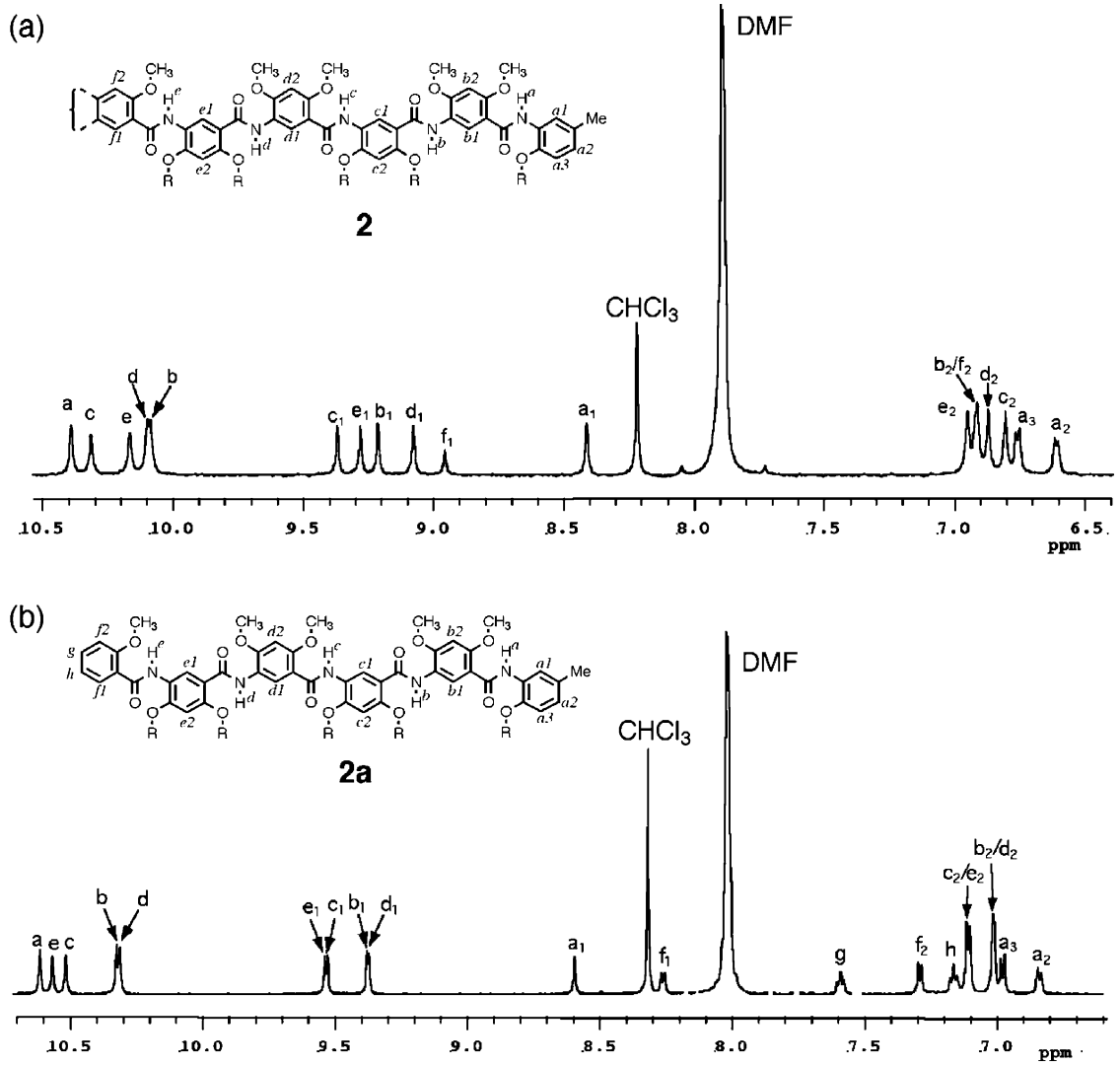

Figure 4. One-dimensional ^{1}H NMR spectra (600 MHz spectrometer equipped with a cryogenic probe, 0.30 mM in 15:85 $CDCl_3$/DMF-d_7, 278 K) of (a) nonamer **2** and (b) hexamer **2a**.

by **2** would be the presence of NOEs between protons on remote residues. The above variable-temperature NOESY experiments on nonamer **1** indicated that, to detect any end-to-end (remote) NOEs, the NOESY experiments need to be carried out at low temperatures. Therefore, the same experimental conditions, which involved room temperature, used to detect the amide−side chain NOEs (Figure 5) were not suitable for studying NOEs between remote protons of **2**. The NOESY experiments were then carried out on a 600 MHz NMR spectrometer at 5 °C. In the resultant NOESY spectrum, the amide and end methyl (Me) protons of **2** were followed to reveal NOEs between nonadjacent protons. These protons were chosen because their signals appeared at positions that were well-separated from those of other protons in the 1D NMR spectrum of **2**. As shown in Figure 6, three sets of NOEs were clearly detected for **2**: one set between amide protons a and b, another between a and aromatic proton c2, and the third between the protons of the end methyl (Me) group and amide proton d. In contrast, similar NOESY study on the reference compound **2a**, which can be regarded as half of **2**, failed to reveal any of the NOEs between the corresponding protons. Therefore, these NOEs revealed in the NOESY spectra of **2** were the result of the approach of the two termini of **2**, which clearly indicated a folded helical conformation that brought the otherwise remote ends into close proximity.

Computer Modeling. We previously determined the crystal structures of a number of crescent oligoamides from dimer **5** up to 9-mer **9** (Figure 7a).[20d,h] The crystal structures of these oligomers provided several sets of parameters, such as bond lengths, bond angles, dihedral angles, and internuclear distances that can serve as structural constraints. On the basis of these parameters, we decided to develop a simple modeling method that may be generally applicable to the prediction of the folded structures of other homologous oligoamides. Such a modeling method would be particularly helpful in predicting the folded structures of long oligomers that are otherwise difficult to characterize by high-resolution methods such as 2D NMR or X-ray crystallography due to signal overlap or the difficulty of growing single crystals. Among the numerous parameters that can be chosen, the distances between the exterior (d_{exterior}) and interior (d_{interior}) aromatic carbons of two neighboring meta-linked benzene rings were tested as distance constraints (Figure 7b). Restraining these two distances in a modeled structure is a direct reflection of the rigidifying effect of the localized three-center H-bonds, which lead to crescent, tapelike backbones.

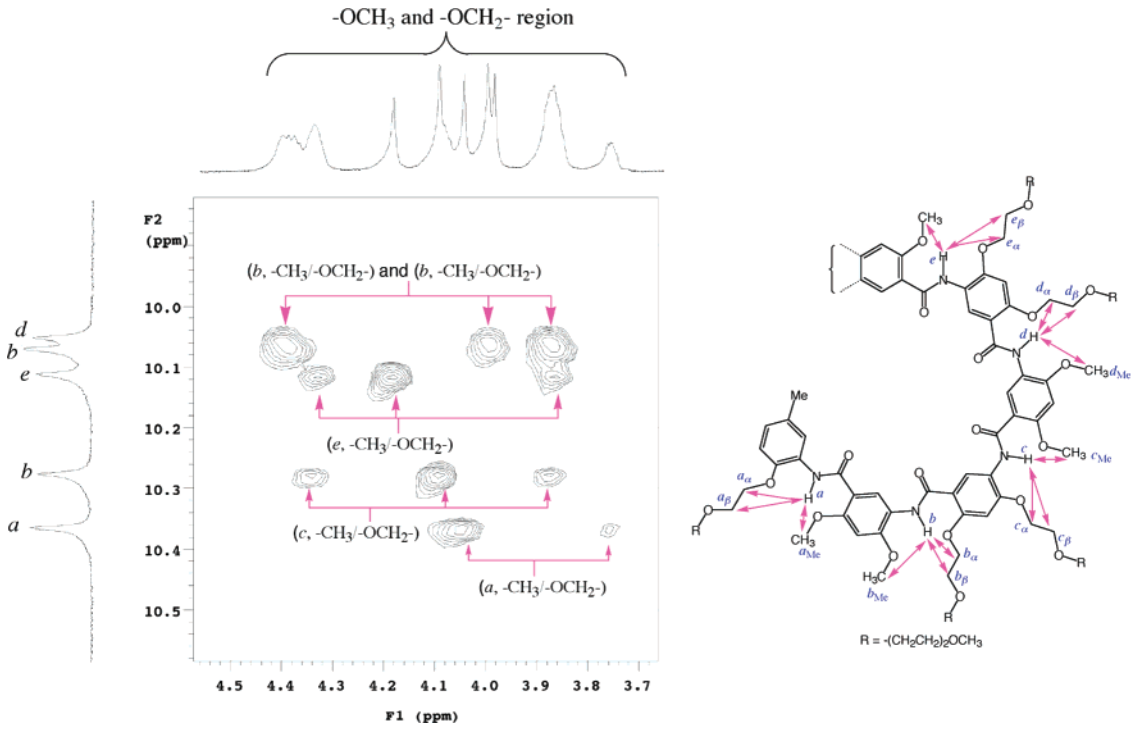

Figure 5. Amide proton−side chain NOEs revealed by the NOESY spectrum of **2** (500 MHz; 0.3 mM in 15:85 $CDCl_3$/DMF-d_7; 298 K; mixing time, 0.4 s).

Specifically, by measuring the two distances based on the crystal structures of oligomers **5**−**9**, average values of 7.812 and 5.384 Å were found for $d_{exterior}$ and $d_{interior}$, respectively. Similar to the calculation of protein structures based on NOE data, "randomly" folded, H-bond-rigidified starting helical structures were first generated for 9-mer **1b** and 11-mer **2b**, respectively, on the basis of the default structural parameters provided by the modeling program ChemBats3D. These two structures, with all of their side groups being methyl, correspond to the backbones of oligomers **1** and **2** described above. The three helical structures were constrained by setting all of the $d_{exterior}$ and $d_{interior}$ with the corresponding average values. The constrained structures were then optimized (MM3 force filed) using the software Cache 3.2, which led to energy-minimized structures as shown in Figure 8. All three computed structures exhibit a helical pitch between 3.5 and 3.6 Å, an interior cavity of ~10 Å across, and about seven residues for a helical turn. These results were consistent with the crystal structure of 9-mer **9** and thus supported the validity of this modeling method.

The reliability of the modeling method was verified by comparing the modeled helical structure of **1b** and **2b** with the experimentally determined remote NOEs for **1** and **2**.

For 9-mer **1** and other 9-mers with the same backbones, an NOE contact between the end methyl (Me) and the second interior aromatic proton b1 have been consistently observed in their NOESY spectra. This Me···b1 contact provides direct evidence for a helical conformation adopted by **1** in solution and, at the same time, suggests that the protons of the end methyl groups and the two protons b1 are brought into close proximity by the folded structure. Indeed, in the modeled structure of **1b**, the protons Me and b1 were found to be the closest among others, with a shortest distance of 3.8 Å and an average of 4.6 Å. Thus, protons Me and b1 were in close proximity for an NOE to be readily detected. In addition, the modeled structure also indicates that one of the three Me protons was 4.16 Å away from amide proton b and the other two Me protons were 5.5 and 5.8 Å away from proton b. This suggest that an NOE may be detected between protons Me and b1. This NOE, in addition to the Me···b1 contact, was indeed found in the NOESY spectrum of a previously characterized nonamer that differs from **1** only in its side groups.[20d] All other nonadjacent groups of protons in the modeled structure of **1b** were found to be too far away for any NOEs to be detected, which was also consistent with results from NOESY studies on **1** and other nonamers.

Table 1. Comparison of Internuclear Distances and the Intensities of the Corresponding Remote NOEs

	internuclear contact		
	Me···Hd	Ha···Hb	Ha···Hc2
H···H distance[a] (Å)	5.513 (av) 4.437 (shortest)	4.843	4.398
NOE intensity[b] (integrated vol)	311.3	760.3	1122.0
relative NOE intensity	1.0	2.4	3.6

[a] Based on the modeled structure of **2b**. [b] From the NOESY spectrum of **2**.

The intensities of the three remote NOEs observed for 11-mer **2** showed excellent correlation with the corresponding internuclear distances revealed by the modeled structure of **2b**. As shown in Table 1, among the three NOEs, the strongest is that between protons a and c2, consistent with which is the internuclear distance between the two protons that was found to be the shortest on the basis of the modeled structure of **2b**; the weakest NOE and the longest (average) H···H distance are found for proton Me and d; and the NOE and H···H distance for protons a and b lies in the middle. The Me···d average distance of 5.513 Å suggests that there should be no detectable NOE between these protons. However, the modeled structure of **2b** shows that one of the three methyl protons can be as

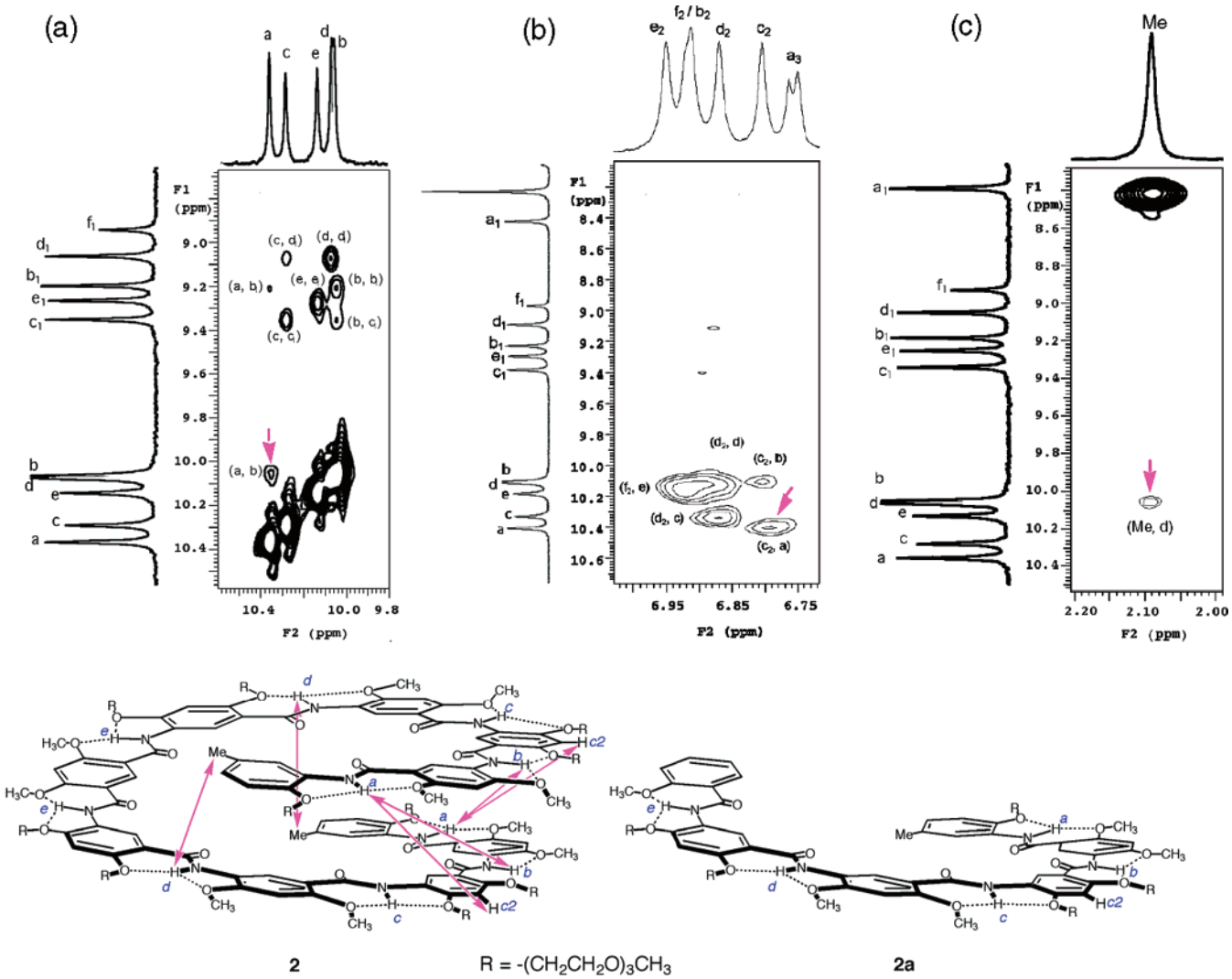

Figure 6. Long-range NOEs revealed by the NOESY spectra of **2** (600 MHz; 0.30 mM in 15:85 $CDCl_3$/DMF-d_7; 278 K; mixing time, 400 ms). The corresponding NOEs were not detected in the NOESY spectrum of **2a** recorded under the same conditions.

close as 4.437 Å away from proton d. Due to the free rotation of the methyl−aryl bond, each of the three methyl protons can lie transiently within distances (<5 Å) from proton d that allow the detection of the NOE, which led to the detection of the weak NOE detected. Thus, the modeled, folded structure of **2b** reflected and explained the observed remote NOEs for **2** rather accurately.

The above comparison between the remote NOEs and modeled internuclear distances clearly showed the reliability of this simple modeling method. We believe it was the well-defined, repetitive backbone structures of our crescent oligoamides that allowed the success modeling of their conformations. The constrained structure of an oligomer based on the average internuclear distances obtained from the crystal structures of short oligomers should represent the average of a series of dynamic conformations of the corresponding oligomer. Such an averaged conformation is in fact the one measured by NMR in solution. Thus, the modeled structure should be particularly useful for the explanation or prediction of structural data obtained from 2D NMR experiments, as already being demonstrated above. By extracting structural parameters from the crystal structures of short oligomers, the concept as illustrated by this simple modeling method should be applicable not only to our backbone-rigidified oligoamides but also to other systems of backbone-rigidified foldamers.

Conclusions

In this paper, the persistence of the three-center H-bonds that play the critical role in maintaining the overall folded conformation of the aromatic oligoamides developed by us has been demonstrated by amide H−D exchange. This method not only serves to quantify the strength of the three-center H-bonds but also provides a convenient measurement of the relative stability of individual three-center H-bonds located at different positions along the backbone of an oligomer. The reliability of the three-center H-bonds leads to well-defined, stably folded, and yet dynamic oligoamide backbones as revealed by 2D NMR. The fact that NOEs between an amide proton and those of its adjacent side chains can be detected even at elevated temperature support the persistence of the three-center H-bonds. Compared to amide−side chain NOEs, the much more rapid disappearance of end-to-end NOEs at elevated temperatures suggests that the distortion of the H-bonded rings associated with each amide group allows the helical structure of the nonamer to extend and breathe like a spring. The numerous remote NOEs detected in the NOESY spectrum of the undecamer demonstrates that longer

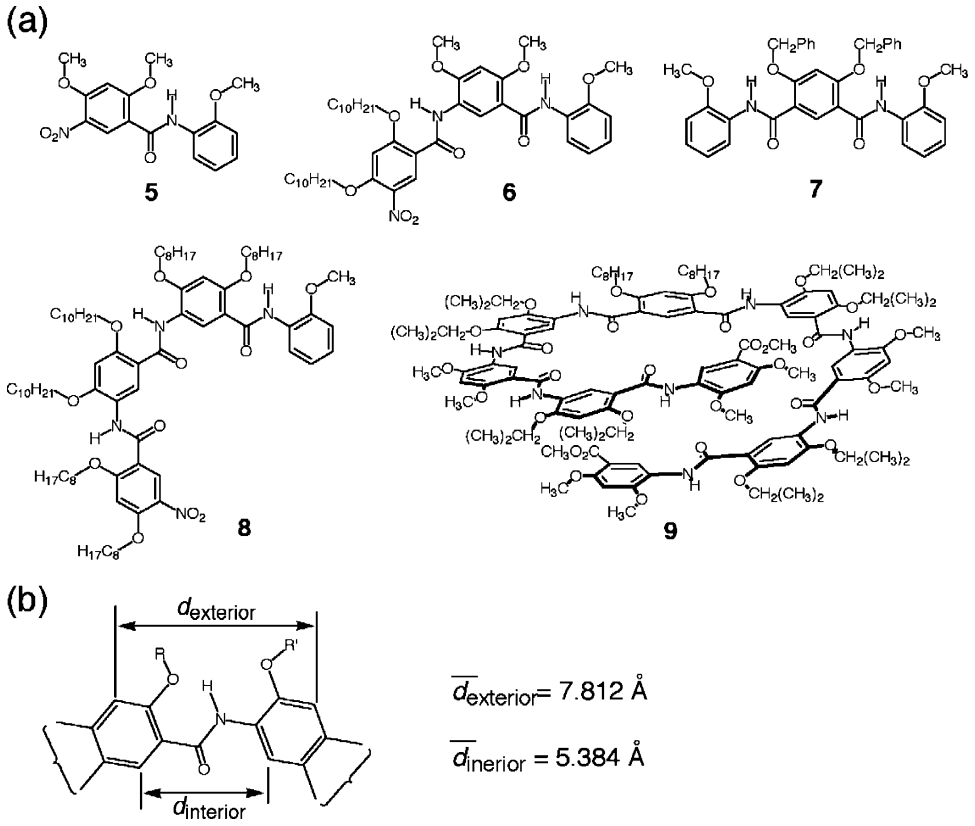

Figure 7. On the basis of (a) the previously determined crystal structures of oligomers **5**−**9**, determination of the average values (b) of distances $d_{exterior}$ and $d_{interior}$.

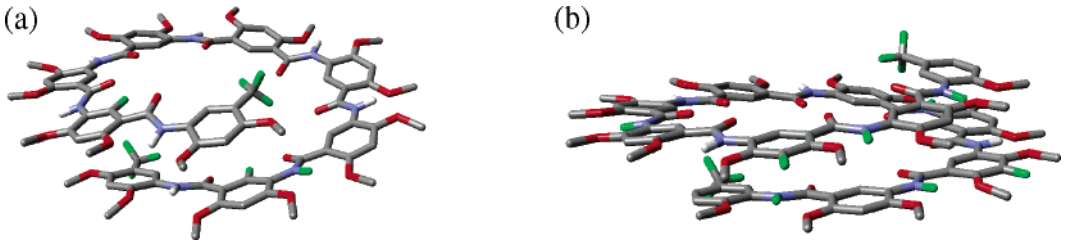

Figure 8. Energy-minimized structures of (a) 9-mer **1b** and (b) 11-mer **2b**. The protons that are involved in remote NOE contacts revealed by the NOESY spectra of **1** and **2** are indicated in green. Except for the indicated and amide protons, all other protons are removed for clarity. The structures were optimized by restraining the distances $d_{exterior}$ and $d_{interior}$ using their corresponding average values obtained from oligomers with known crystal structures (see Figure 8).

oligomers also fold predictably into helical conformation in solution. Finally, predictability of the folded conformations of these aromatic oligoamides is demonstrated by the excellent agreement between the modeled structures and results from NOESY studies. The modeling method should be particularly useful for future design of long oligomers that are difficult to characterize by methods such as NMR and X-ray crytstallography. The modeling method described here should be generally applicable to the prediction of folded structures of other backbone-rigidified oligomers when the crystal structures of short oligmers are known.

Experimental Section

General Methods. All reactions were performed under argon. All chemicals were obtained from commercial suppliers and were used as received unless otherwise noted. CH_2Cl_2 was dried over CaH_2. Unless otherwise specified, all solvents were removed with a rotary vacuum evaporator. Analytical thin-layer chromatography (TLC) was conducted on Analtech Uniplate silica gel plates with detection by UV light. NMR analyses were carried out on a Varian INOVA 500 spectrometer (500 MHz). Tetramethylsilane (TMS) or deuterated solvent DMSO-d_6 was used as the internal standard for ^{1}H NMR. Chemical shifts are reported in parts per million values downfield from tetramethylsilane, and J values are reported in hertz. MALDI-TOF MS spectra were recorded on a Bruker Biflex IV MS spectrometer with dithranol as a matrix. Electrospray ionization (ESI) mass spectra were obtained by Themo Finnigan LCQ Advantage mass spectrometer.

Nonamer 1. This oligomer was obtained in 51% on the basis of the same procedures reported by us before for preparing nonamer **1a**.[20d] ^{1}H NMR (500 MHz, 285 K, DMF-d_7): δ 10.38 (s, 2H), 10.36 (s, 2H), 10.17 (s, 2H), 9.93 (s, 2H), 9.39 (s, 2H), 9.33 (s, 2H), 9.23 (s, 2H), 9.00 (s, 2H), 8.40 (s, 2H), 7.00 (s, 2H), 6.95 (s, 1H), 6.93 (s, 2H), 6.89 (s, 2H), 6.80 (d, J = 8.5 Hz, 2H), 6.59 (d, J = 8.0 Hz, 2H), 4.44 (t, 4H), 4.39 (m, 8H), 4.13 (s, 6H), 4.12 (t, 4H), 4.08 (s, 6H), 4.04 (s, 6H), 4.02 (s, 6H), 3.90 (m, 8H), 3.78 (t, 4H), 3.25−3.60 (m, side chains), 3.14, 3.13, 3.10 (s, s, s, 18H), 2.50 (t, J = 7.5 Hz, 4H), 2.17 (q, 4H), 2.06 (s, 6H). MALDI-TOF MS m/z. Calcd for $C_{126}H_{170}N_8O_{46}$-Na ($M + Na^+$): 2554.11. Found: 2554.5.

Undecamer 2. This oligomer was synthesized by coupling 4,6-dimethoxyisophthaloyl choride[24] with the corresponding amino-pentamer that was prepared by stepwise (C-to-N) coupling of the

corresponding monomer building blocks based on acid chloride chemistry. Specifically, 4,6-dimethoxyisophthaloyl choride, obtained from 4,6-dimethoxyisophthalic acid (24.0 mg, 0.106 mmol) and oxalyl chloride (0.134 g, 1.06 mmol) in dry CH_2Cl_2 (5 mL), was added dropwise at room temperature to the CH_2Cl_2 (20 mL) solution of the amino-pentamer (320 mg, 0.22 mmol). The mixture was stirred overnight. The reaction mixture was worked up by using column chromatography (silica gel, $CHCl_3$/EtAc/MeOH = 5:2:3), which afforded 0.15 g of faint-yellow solid (42.4%). Preparative TLC separation ($CHCl_3$/EtAc/MeOH = 10:2:4) gave a pure yellow crystal suitable for analysis. ^{1}H NMR (500 MHz, 273 K, 20/80 DMSO-d_6−$CDCl_3$): δ 10.37 (s, 2H), 10.10 (s, 2H), 10.08 (s, 2H), 9.92 (s, 2H), 9.98 (s, 2H), 9.29 (s, 2H), 9.25 (s, 2H), 9.14 (s, 2H), 9.03 (s, 1H), 8.98 (s, 2H), 8.48 (s, 2H), 6.60−6.73 (m, 8H), 6.66 (s, 1H), 6.59 (s, 2H), 6.53 (s, 2H), 3.24−4.38 (m, side chains), 2.26 (s, 6H). MALDI TOF MS *m*/*z*. Calcd for $C_{158}H_{220}N_{10}O_{60}Na$ ($M + Na^+$): 3240.43. Found: 3240.3.

Hexamer 2a. This compound was obtained in 78% yield on the basis of the similar procedures for preparing 11-mer **2** by acylating the corresponding amino-pentamer with anisoyl chloride. ^{1}H NMR (500 MHz, 273 K, 20:80 DMSO-d_6/$CDCl_3$): δ 10.49 (s, 1H), 10.42 (s, 1H), 10.31 (s, 1H), 10.08 (s, 1H), 10.06 (s, 1H), 9.35 (s, 1H), 9.34 (s, 1H), 9.19 (s, 1H), 9.16 (s, 1H), 8.54 (s, 1H), 8.30 (d, 1H), 7.54 (t, J = 8.5 Hz, 1H), 7.14 (t, J = 8.0 Hz, 1H), 7.11 (d, J = 8.0 Hz, 1H), 6.84 (m, 2H), 6.75 (s, 1H), 6.71 (s, 1H), 6.66 (s, 1H), 4.41−4.36 (m, 8H), 4.26 (t, 2H), 4.14 (s, s, 6), 4.12 (s, 3H), 4.07 (s, 3H), 4.04 (s, 3H), 3.98−4.00 (m, 8H), 3.94 (t, 2H), 3.44−3.77 (m, side chains), 2.35 (s, 3H). ESI MS *m*/*z*. Calcd for $C_{82}H_{114}N_5O_{30}$ ($M + H)^+$: 1648.75. Found: 1649.0.

Two-Dimensional NMR Spectroscopy. NMR experiments were recorded on Varian Inova 500 and 600 spectrometers, processed, and analyzed with the program VNMR 6.1C. The 600 MHz machine is equipped with a cryogenic probe. Temperatures in the probe of spectrometers were calibrated with use of the ^{1}H resonances of methanol. [^{1}H,^{1}H]-NOESY spectra[25] of **1** were recorded at a 500 MHz ^{1}H spectrometer frequency with a mixing time, τ_{mix}, of 150−500 ms and at T (sample) of −10, −5, 0, 15, and 21 °C in $CDCl_3$, and from 200 to 54 ms and at T (sample) of −20, −10, −5, 0, 10, and 21 °C in DMF-d_7 for 14−20 h. The NOESY spectrum of **2** was recorded at a 600 MHz ^{1}H spectrometer frequency with a mixing time of 400 ms for 8 h. τ_{mix} at different temperature was scaled with $1/\tau_c$, where τ_c represents the correlation time for the overall rotational tumbling estimated as described.[26] It needs to be pointed out that these 2D NMR measurements on **2** would not be possible without the sensitivity provided by the cryogenic probe which allows the spectra to be recorded before the molecules precipitated out.

Amide H−D Exchange. Solutions of **1a**, **3**, **3a**, and **3b** (2 mM) were prepared by dissolving the compounds into 50% DMSO-d_6 in $CDCl_3$ (total volume: 0.95 mL) and the spectra were recorded at room temperature as the reference spectra at t = 0. The H−D exchange experiments were initiated by adding 0.05 mL of D_2O into each of the samples, which resulted in a solution in a mixed solvent of 5:47.5:47.5 D_2O/DMSO-d_6/$CDCl_3$. The resultant spectra were then recorded (500 MHz) at appropriate time intervals, based on which the time-dependent peak areas of the amide protons were obtained and fitted into the pseudo-first-order reaction rate equation of $(I_t - I_\infty)/(I_o - I_\infty) = e^{-kt}$, where I_t, I_∞, and I_0, correspond to the integrated area of the corresponding proton at $t = t$, $t = \infty$, and $t = 0$; k is the decay rate constant. The half-life $T_{1/2}$ is related to k by $T_{1/2} = \ln 2/k$. Thus, the half-life $T_{1/2}$ was obtained by fitting the time-dependent peak areas into the above equation [$(I_t - I_\infty)/(I_o - I_\infty) = e^{-kt}$] with the program Kaleidagraph on a Macintosh computer.

Acknowledgment. This work was supported by grants from NIH (R01GM63223), ONR (N000140210519), and NSF (CHE-0314577).

JA046858W

(24) (a) Zeng, H.; Miller, R.; Flowers, R. A.; Gong, B. *J. Am. Chem. Soc.* **2000**, *122*, 2635. (b) Gong, B.; Yan, Y.; Zeng, H. Q.; Skrzypczak-Jankunn, E.; Kim, Y. W.; Zhu, J.; Ickes, H. *J. Am. Chem. Soc.* **1999**, *121*, 5607.

(25) Ernst, R. R.; Bodenhausen, G.; Wokaun, A. *Principles of Nuclear Magnetic Resonance in One and Two Dimensions*; Clarendon Press: Oxford, U.K., 1987.

(26) Skalicky, J. J.; Mills, J. L.; Sharma, S.; Szyperski, T. *J. Am. Chem. Soc.* **2001**, *123*, 388.